

# An Approach to Reaction Path Branching using Valley-Ridge-Inflection Points of Potential Energy Surfaces

---

Wolfgang Quapp

*Mathematisches Institut, Universität Leipzig, Augustus-Platz 04109 Leipzig*

quapp@rz.uni-leipzig.de

Web: [www.mathematik.uni-leipzig.de/MI/quapp](http://www.mathematik.uni-leipzig.de/MI/quapp)

**Key words:** Reaction path following – Projected gradient – Gradient extremal – Valley-ridge-inflection point

- Valley-ridge-inflection points (VRI) of a potential energy surface (PES) may have a strong relation to the occurrence of bifurcations along chemical reaction paths.
- The calculation of symmetric VRI points has been already reported: [W.Quapp et al., TCA 100 (1998) 285-299].
- We calculate special asymmetric VRI points which are placed on gradient extremals (GE). Following a GE opens the possibility to find the VRI point on it.
- The method is based on a mathematical connection between the following of a reduced gradient (RGF) and the calculation of GEs.
- The tangent search method to follow a GE to the smallest eigenvalue [W.Quapp et al., TCA 105 (2000) 145-155] is extended to follow also GEs to higher eigenvalues in order to find a VRI point.
- The new method needs gradient and second derivatives of the PES only.

## 1 Why it is difficult to find a ‘lop-sided’ VRI point?

It is a common assumption that a transition state of a chemical reaction connects two minima of the PES. However, this simple definition does not exclude more complex courses of reactions passing additional saddle points between reactant and product. A sample PES can be described by a valley descending from the higher energy saddle point leading into another (‘orthogonal’) valley:

$$E(x, y) = \frac{1}{2} (xy^2 - yx^2 - \mu x + 2y) + \frac{1}{30} (x^4 + y^4). \quad (1)$$

We use  $\mu=2, 1.75, 1,$  and  $0.5$  to generate a sequence of ‘orthogonal’ valleys.

**Figure 1** starts with the symmetric case,  $\mu = 2$ . Two saddle points with orthogonal valleys are shown. An IRC leads from  $SP_1$  to  $SP_2$ . The IRC here coincides with a GE. Note that three minima of the surface exist outside the Figure where the minimum above left is considered as reactant, and the two other minima shall represent the two products.

Near  $SP_2$ , the IRC leads down along a ridge. The point  $(0,0)$  where the first valley ends, and meets the ridge, is the valley-ridge inflection point.

**Definition 1** *A VRI point is that point where, orthogonally to the gradient, at least one main curvature of the PES becomes zero. This has two conditions:*

- (i) one eigenvalue of the Hessian must be zero, and*
- (ii) the gradient is orthogonal to the corresponding zero-eigenvector.*

VRI points in the narrow sense of definition 1 are given independently of a reaction path definition. The VRI point is a bifurcation point, from which reaction paths may lead to one of two product minima. However, the IRC does not follow the reaction path branching. Both, IRC and GE do not reflect that there are two valleys besides the ridge leading to the two product minima. If (and only if) the symmetry is enforced during the calculation, the IRC would be the method of choice to calculate the symmetric VRI point: by taking an additional test of the eigenvalues along the path. We stop if we find a zero eigenvalue belonging to an orthogonal eigenvector.

The reaction path of Figure 1 splits into two branches complicating the identification of the reaction path model. The IRC leads from  $SP_1$  to  $SP_2$  and splits orthogonally into two branches to the two minima. This combined, ‘cornered’ pathway is not the ‘shortest’ one. But in Figure 1, also a special RGF curve is included. One branch of the RGF also coincides with the IRC from  $SP_1$ . At every point on this curve, the gradient of the PES has the same direction  $(-1,1)$ . The RGF curve has a bifurcation point at the VRI point and the bifurcating branches reflect the symmetry break of the PES. One may consider the RGF curve as a model of a reaction path. Again, we have the problem of a ‘cornered’ reaction path model. Nevertheless, this pathway is ‘shorter’ than the IRC from  $SP_1$  to minimum via the  $SP_2$ .

**Figure 2** shows a slightly disturbed symmetry of the surface (1) using parameter  $\mu = 1.75$ . The IRC directly leads from  $SP_1$  to the left hand deeper valley below, but the GE further follows the crest of the ridge to connect the two saddle points. The VRI point again is at  $(0,0)$  on the GE; it is not on the IRC from  $SP_1$ .

A question emerges: is there a point in Figure 2 where the steepest descent meets a direction with zero curvature of the PES being orthogonal to the gradient? The answer is: yes, it happens at the point where the IRC meets the border of the ridge region. That border is the thin dashed line defined by

$$\boxed{\mathbf{g}^T \mathbf{A} \mathbf{g} = 0} \quad (2)$$

where  $\mathbf{g}$  is the gradient of  $E$ , and  $\mathbf{A}$  is the adjoint matrix to the Hessian,  $\mathbf{H}$ .  $\mathbf{A}$  is defined as  $((-1)^{i+j} m_{ij})^T$  where  $m_{ij}$  is the minor of  $\mathbf{H}$  obtained by deletion of the  $i^{th}$  row and the  $j^{th}$  column from  $\mathbf{H}$ , and taking the determinant. At the border, of course, a valley-ridge transition occurs.

**Definition 2:** *A valley-ridge transition point on the IRC is the first intersection of the IRC with the manifold of solutions of eq.(2).*

There, the gradient is not orthogonal to one of the eigenvectors of the PES, in the general case, and both of the two eigenvalues are not zero. The zero curvature of the PES along the level line comes from a suitable linear combination of the two eigenvalues. The points on that border do not fulfill the narrow definition 1 of the VRI point, in the general case.

In Fig.2 we include couples of eigenvectors of the PES to be able to compare the gradient and the eigenvectors of the Hessian. Along the IRC, there does not exist a VRI point with the definition 1. But the IRC goes through a region of the ridge. Due to this fact, one has to conclude that there is a valley-ridge transition with definition 2. Understanding the IRC from  $SP_1$  to be the reaction path then there is no reaction path bifurcation at the valley-ridge transition.

The special RGF curve to the gradient direction  $(-\mu,2)$  with  $\mu=1.75$  is also included in Figure 2. It is that curve which here has a bifurcation point at the VRI point, and which may serve as a reaction path model alternately to the IRC.

**Figure 3** shows a further extension of eq.(1) to the more asymmetric lop-sided VRI case with  $\mu = 1$ . Again, the VRI point is at  $(0,0)$  on the GE, which again connects  $SP_1$  and  $SP_2$ . The GE curve carries the valley-ridge inflection. However, the IRC early deviates from this GE by going downhill the slope to the deeper minimum.

The symmetry is so strongly disturbed that the IRC does not meet the ridge region. However, there is a ‘remainder’ of a valley-ridge transition near the VRI point. We show two steepest descent lines (‘meta-IRCs’) which include this region (bullet lines). They come from a valley region with convex behavior of the PES and they pass the ridge region with concave behavior.

Included in Fig.3 is again the border (2) between valley and ridge of the PES (dotted lines). A curve like the GE from  $SP_1$  over VRI to  $SP_2$  usually is assumed to be not a ‘reaction path’ model because steepest descent lines from above intersect the GE under large crossing angles. However, a dynamically favored non-steepest-descent path from  $SP_1$  may directly find the second minimum at the right hand side of Figure 3.

The special RGF curve with constant gradient direction  $(-\mu,2)$  with  $\mu=1$  is included in Fig.3. This curve has a bifurcation point at the VRI point and also passes the  $SP_2$ . It may serve as a reaction path model.

**Figure 4** refers to the case of eq.(1) with  $\mu = 0.5$ . It is a further extension of the asymmetry of the PES. The qualitative description is equal to that of Figure 3. However, The GE between the downward valley of  $SP_1$  and the uphill crest of  $SP_2$  shows two turning points (TP). So, the structure of the GE becomes more complicate.

$TP_1$  marks the end of the valley of  $SP_1$  where  $TP_2$  marks the end of the ridge of  $SP_2$ . The VRI point is only a point of the border between the ridge above and the valley below. But also in this case there is the VRI point  $(0,0)$  on the GE. We conclude that there is a border between the steepest descent valley through  $SP_1$  and the steepest ascent ridge through  $SP_2$ . The existence of the  $TP_1$  forms a qualitative important valley characterization. The steepest descent, as well as a family of RGF curves through  $SP_1$  estimate the reaction channel to the minimum below. This family of RGF curves is bounded by the special RGF curve to the constant gradient search direction  $(-\mu,2)$  with  $\mu=0.5$ . It is the curve which has a bifurcation point at the VRI point. It may serve as a reaction path model.

It is plausible that the IRC from  $SP_1$  in Figures 2 to 4 does not find the VRI point. However, there is in every case a special RGF curve which leads to the VRI point. This curve could be obtained, in our case, by trial and error. However, in more than 2 dimensions, there is no straight-forward method to find the special RGF curve which bifurcates at a lop-sided VRI point.

The only direct way is to follow the GE. A strategy to follow a GE is already given by Sun and Ruedenberg (1993) [Gradient extremals and steepest descent lines on potential energy surfaces] J Chem Phys 98: 9707-9714; but the method needs some third derivatives of the PES. This will be avoided in the procedure of section 5.

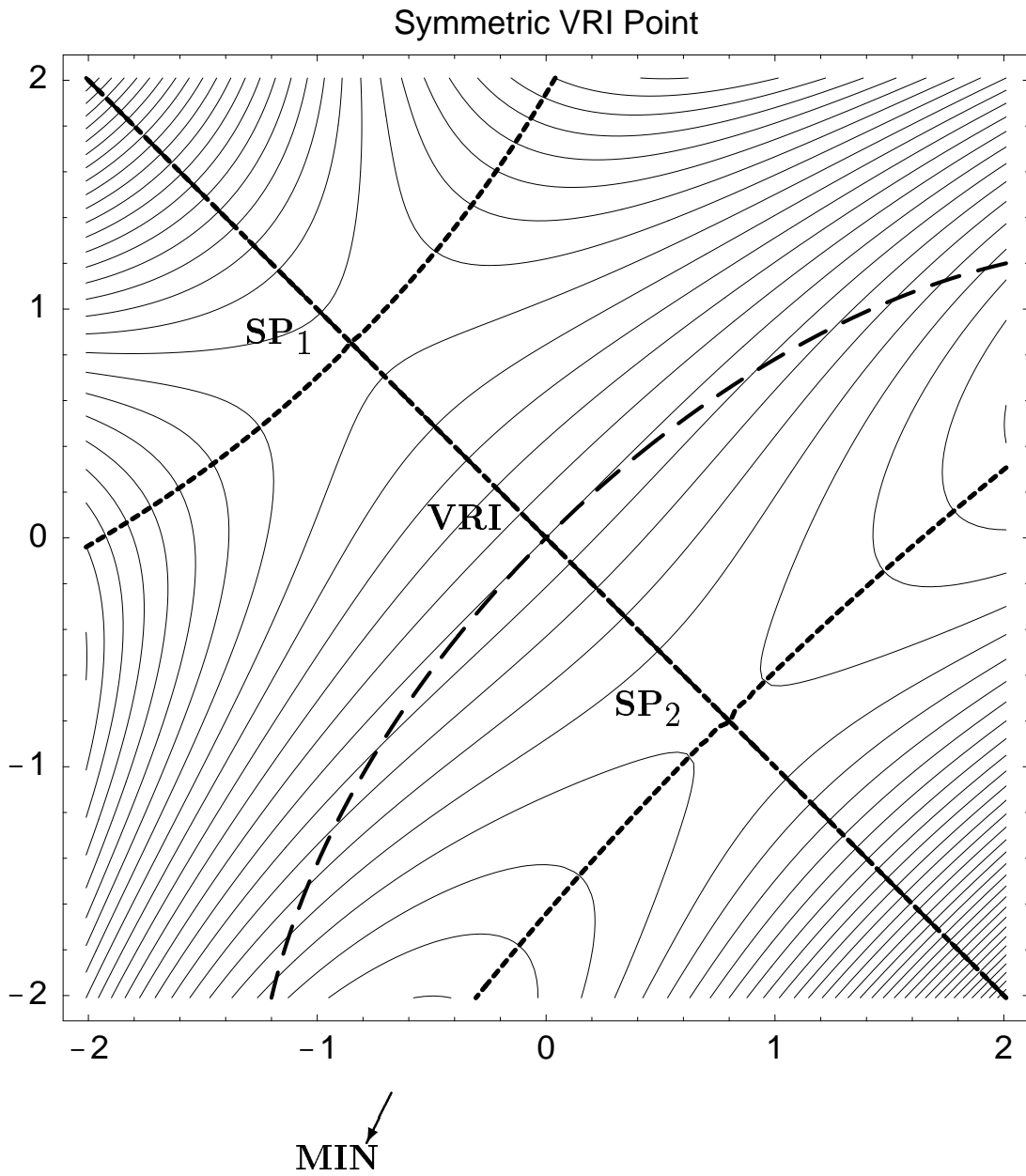


**FIGURE 1.**  
 Equipotential lines of model potential energy surface (1) with  $\mu=2$ . GEs are dotted thick curves, RGFs are bold dashes. (The diagonal line is GE, RGF, as well as IRC.) The valley-ridge-inflection point (VRI) is at (0,0).

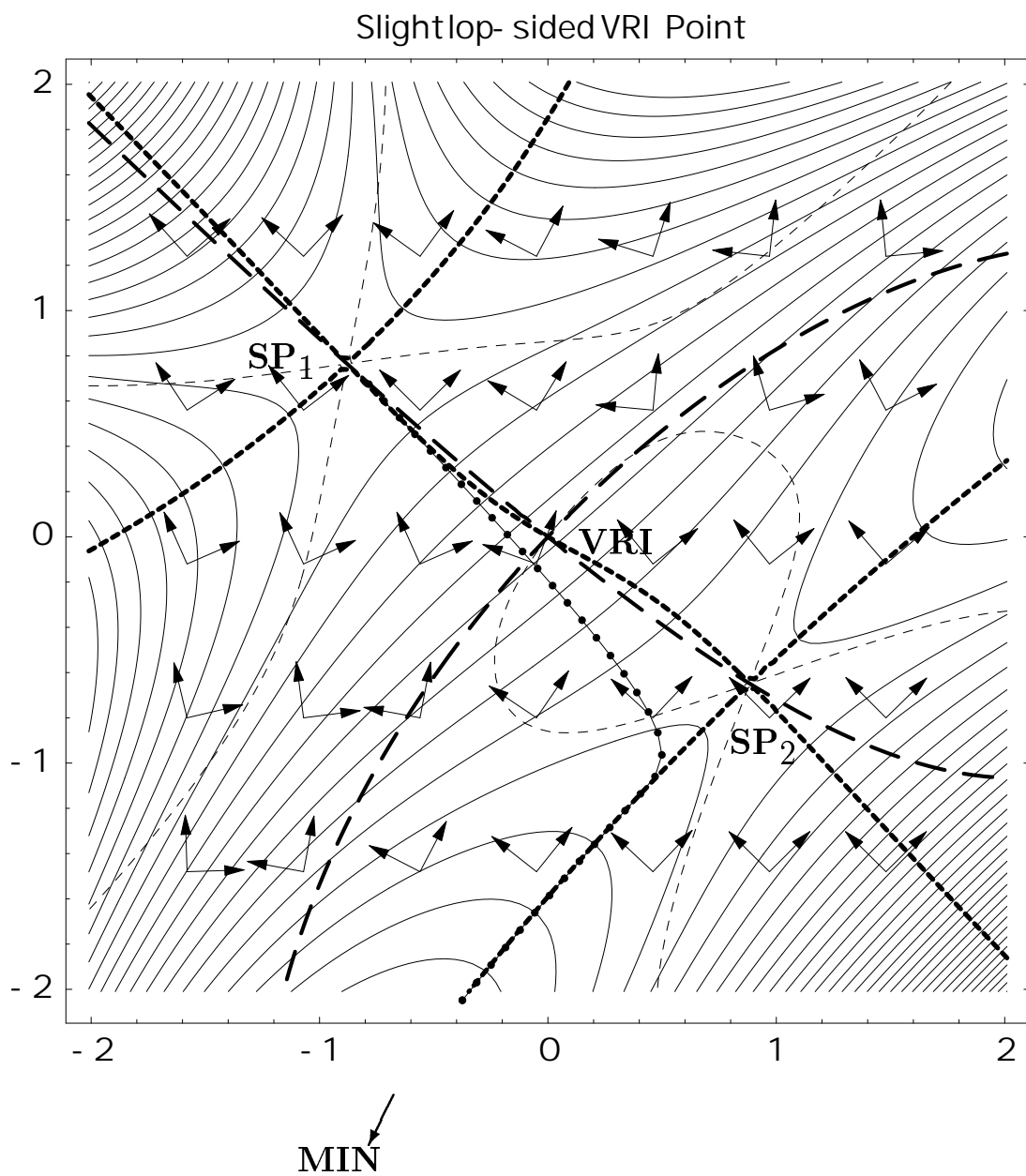


**FIGURE 2.**  
 Equipotential lines of 2D model PES (1) with  $\mu=1.75$ . The IRC from  $SP_1$  is the line with dots. GEs are dotted thick curves, RGFs are bold dashes. Pairs of eigenvectors of the Hessian are shown at a grid of points. Thin dashed lines are the border (2) between valley and ridge of the PES.

## 2 Following the Projected Gradient (RGF)

We start at the solution of

$$\nabla E(\mathbf{x}) = \mathbf{0}, \quad \mathbf{x} \in \mathbb{R}^n, \quad (3)$$

a stationary point of  $E$ . By  $\mathbf{g}(\mathbf{x}) := \nabla E(\mathbf{x})$  we denote the gradient vector of  $E$ . We choose a search direction  $\mathbf{r}$  being a unit column vector and define a projector,  $\mathbf{P}_r$ , by the dyadic product

$$\mathbf{P}_r := \mathbf{I}_n - \mathbf{r}\mathbf{r}^T \quad (4)$$

using the  $n$ -dimensional unit matrix  $\mathbf{I}_n$ . The projector realizes  $\mathbf{P}_r \mathbf{r} = \mathbf{0}$ . It is a constant matrix of rank  $(n-1)$ . If there is a point  $\mathbf{x}$  where the gradient  $\mathbf{g}(\mathbf{x})$  fulfills the system of projector equations

$$\boxed{\mathbf{P}_r \mathbf{g}(\mathbf{x}) = \mathbf{0}} \quad (5)$$

then this gradient is named the *reduced gradient with respect to the direction  $\mathbf{r}$* .

Solutions of the eq.(5) connect stationary points which differ in their index by one, if no bifurcation point is crossed. We numerically follow the curve (5) by tangent continuation. We use a predictor-corrector method. The tangent to curve (5),  $\mathbf{x}'(t)$ , is obtained by the derivative to the curve parameter

$$\mathbf{0} = \frac{d}{dt}[\mathbf{P}_r \mathbf{g}(\mathbf{x}(t))] = \mathbf{P}_r \frac{d\mathbf{g}(\mathbf{x}(t))}{dt} = \mathbf{P}_r \mathbf{H}(\mathbf{x}(t)) \mathbf{x}'(t). \quad (6)$$

In general, the search direction,  $\mathbf{r}$ , and the tangent,  $\mathbf{x}'(t)$ , to the RGF curve with respect to  $\mathbf{r}$  are different. The *predictor-corrector method of RGF* is the predictor step along the tangent  $\mathbf{x}'(t)$ , and Newton-Raphson steps of the corrector to search (usually orthogonal to this direction) a solution of curve (5). The simplicity of RGF is based on the constance of the  $\mathbf{P}_r$  matrix which is intrinsically used in eq.(6).

Like steepest descent curves, also RGF curves form a dense family of curves in the coordinate space.



### 3 Gradient Extremal (GE)

Be  $\mathbf{g}(\mathbf{x}) \neq \mathbf{0}$ , and we assume to be on a ‘valley ground’ of the PES. A point showing the gentlest ascent of the valley is defined by the condition that the norm of the gradient forms a minimum taken along an equi-subsurface,  $L_c := \{\mathbf{x} | E(\mathbf{x}) = c\}$  where  $c$  is constant, i.e. in all directions perpendicular to the gradient. The measure for the ascent of the PES,  $E(\mathbf{x})$ , is the norm of the gradient vector

$$\sigma(\mathbf{x}) := \frac{1}{2} \|\mathbf{g}(\mathbf{x})\|^2 . \quad (7)$$

The implicit condition  $E(\mathbf{x}) = c$  may be fulfilled by the sub-hypersurface  $\mathbf{x}(\mathbf{u}, c)$ , where  $\mathbf{u}$  may be an  $(n-1)$ -dimensional parameter. We treat the parametric optimization problem to minimize  $\sigma(\mathbf{x})$  subject to  $\mathbf{x} \in L_c$

$$\sigma(\mathbf{x}) \rightarrow \underset{\mathbf{x}(\cdot, c)}{Min} ! \quad (8)$$

where the nonlinear constraint is  $E(\mathbf{x}) = c$ . Thus, the function to optimize and the constraint are developed from the PES itself. We are interested in following a path of local minima as the parameter increases (if we do an ascent on the surface) or decreases (if we go downhill). Using the normalized gradient

$$\mathbf{w}(\mathbf{u}, c) := \mathbf{g}(\mathbf{x}(\mathbf{u}, c)) / \|\mathbf{g}(\mathbf{x}(\mathbf{u}, c))\| \quad \text{and} \quad \mathbf{P}_{\mathbf{w}(\mathbf{u}, c)} := \mathbf{I} - \mathbf{w}(\mathbf{u}, c) \mathbf{w}(\mathbf{u}, c)^T , \quad (9)$$

the requirement for an extremal value of  $\sigma$  is expressed by

$$\mathbf{P}_{\mathbf{w}(\mathbf{u}, c)} \nabla \sigma(\mathbf{x}(\mathbf{u}, c)) = 0 , \quad \text{with } c = \text{constant} . \quad (10)$$

Because of  $\nabla \sigma(\mathbf{x}) = \mathbf{H}(\mathbf{x}) \mathbf{g}(\mathbf{x})$ , and setting  $\lambda := \mathbf{w}^T \mathbf{H} \mathbf{w}$  for the Rayleigh quotient, it results in the basic eigenvector relation for a gradient extremal

$$\boxed{\mathbf{H}(\mathbf{x}) \mathbf{g}(\mathbf{x}) = \lambda(\mathbf{x}) \mathbf{g}(\mathbf{x})} \quad (11)$$

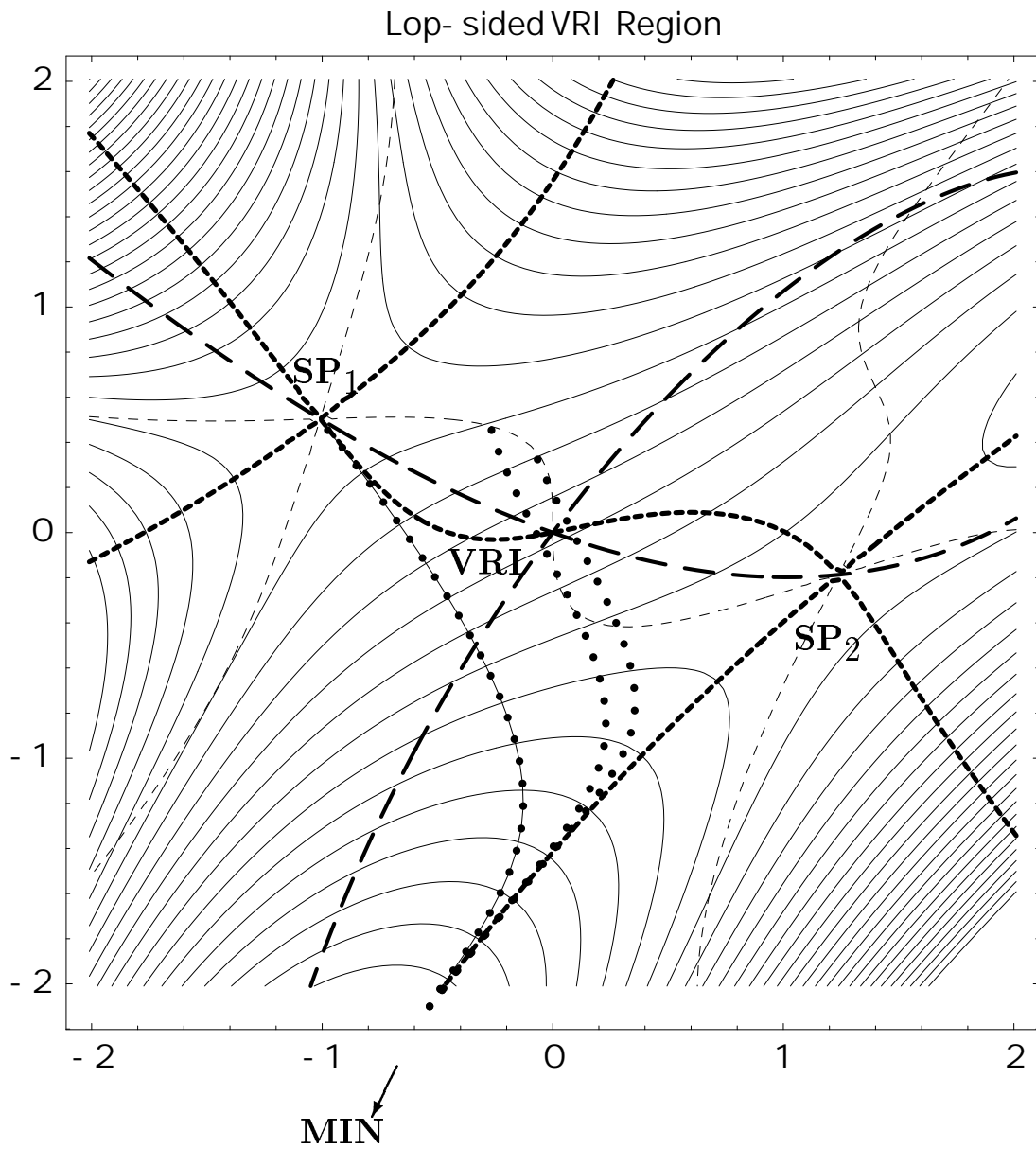


**FIGURE 3.**  
 Equipotential lines of model PES (1) with  $\mu=1$ . The IRC from  $SP_1$  is the line with dots, and two further steepest descent lines are given by dots. They go from valley to ridge: the thin dashed lines are the border (2) between valley and ridge of the PES.

### AsymmetricVRI Point

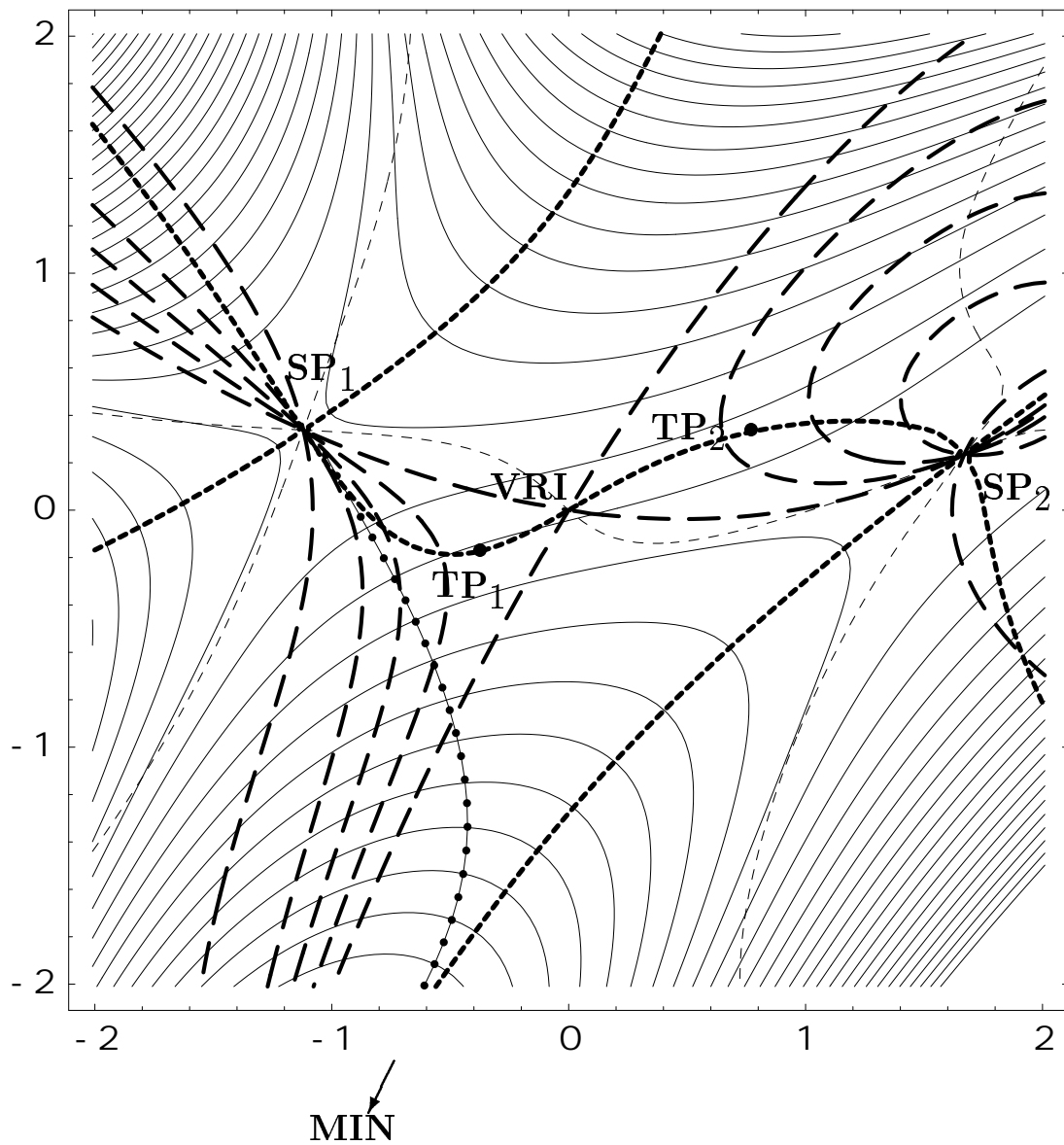


**FIGURE 4.**

Equipotential lines of model PES (1) with  $\mu=0.5$ . A family of RGF curves (bold dashes) is additionally shown where corresponding branches lead from  $SP_1$  to  $MIN$ . TPs are turning points of the GE from  $SP_1$  to  $VRI$  to  $SP_2$ .

### 3.1 Relation between GE and RGF

*A point  $\mathbf{x}$  where the tangent of an RGF curve through this point is parallel to the gradient belongs to a gradient extremal.*

The proof is easy. If  $\mathbf{e}_1, \dots, \mathbf{e}_n$  are the eigenvectors of  $\mathbf{H}$  with eigenvalues  $\lambda_1, \dots, \lambda_n$  then they are also the eigenvectors of the adjoint matrix,  $\mathbf{A}$ , but with the eigenvalues  $\mu_i = \prod_{j \neq i} \lambda_j$ . This is due to the equation  $\mathbf{H} \mathbf{e}_i = \lambda_i \mathbf{e}_i$ , and, by multiplication with  $\mathbf{A}$ , we get

$$\mathbf{A} \mathbf{H} \mathbf{e}_i = \text{Det}(\mathbf{H}) \mathbf{e}_i = \lambda_i \mathbf{A} \mathbf{e}_i, \quad \text{with } \text{Det}(\mathbf{H}) = \prod_{j=1}^n \lambda_j. \quad (12)$$

The gradient is eigenvector of  $\mathbf{H}$  and also of  $\mathbf{A}$  on a GE. RGFs are also solutions of the differential equation of Branin by

$$\frac{d\mathbf{x}}{dt} = \mathbf{x}'(t) = \pm \mathbf{A}(\mathbf{x}(t)) \mathbf{g}(\mathbf{x}(t)). \quad (13)$$

This gives the proof.

### 3.2 Relation between GE and VRI

The definition of a GE is that the gradient is itself an eigenvector of the Hessian. It is clear by definition 1 that, *if another eigenvector becomes a zero eigenvector, the point of the GE where this happens is a VRI point.* Walking along a GE from a convex to a concave region, where an orthogonal eigenvalue has to change its sign, must lead to a VRI point.

Vice versa, *if a GE intersects the convexity border (2) then it meets a VRI point.* There the gradient is eigenvector of  $\mathbf{H}$  with eigenvalue  $\lambda_1$ , and the gradient also is eigenvector of  $\mathbf{A}$  with eigenvalue  $\mu = \prod_{j=2}^n \lambda_j = 0$ . To fulfill eq.(2), one of the  $\lambda_j$ ,  $j = 2, \dots, n$  has to be zero, the corresponding eigenvector orthogonal to the gradient is the zero eigenvector.

## 4 Following the Tangent of the Previous Predictor Step

We change the projector of RGF after every predictor step: the tangent direction of the previous curve point, from eq.(6), iteratively becomes the search direction used in the projector. The procedure is named the TAngent Search Concept (**TASC**).

(The task is: find the valley floor line!) But the calculations of the predictor-corrector method of the former RGF were continued to do.

### **TASC step:**

Assume we are at  $\mathbf{x}_k$  with  $\mathbf{g}(\mathbf{x}_k)/\|\mathbf{g}(\mathbf{x}_k)\| = \mathbf{r}_k$ , where  $\mathbf{r}_k$  is RGF search direction.

(i) Solve former eq.(6):

$$\mathbf{P}_{\mathbf{r}_k} \mathbf{H}(\mathbf{x}_k) \mathbf{x}'_k = 0, \quad (14)$$

to get the tangent direction  $\mathbf{t}(\mathbf{x}_k) = \mathbf{x}'_k/\|\mathbf{x}'_k\|$  for the predictor step to an RGF curve with respect to  $\mathbf{r}_k$ , and do the step to  $\mathbf{x}_k \pm s_k \mathbf{t}(\mathbf{x}_k)$ . The  $s_k$  is a step length.

(ii) Change the search direction to  $\mathbf{r}_{k+1} = \mathbf{x}'_k/\|\mathbf{x}'_k\|$  and compute  $\mathbf{P}_{\mathbf{r}_{k+1}}$  to solve the modified equation

$$\mathbf{P}_{\mathbf{r}_{k+1}} \mathbf{g}(\mathbf{x}) = 0 \quad (15)$$

(instead of  $\mathbf{P}_{\mathbf{r}_k} \mathbf{g}(\mathbf{x}) = 0$ ) by Newton-Raphson steps  $\Delta \mathbf{x}^i$

$$(\mathbf{P}_{\mathbf{r}_{k+1}} \mathbf{H}(\mathbf{x}^i)) \Delta \mathbf{x}^i = -\mathbf{P}_{\mathbf{r}_{k+1}} \mathbf{g}(\mathbf{x}^i), \quad \mathbf{x}^{i+1} = \mathbf{x}^i + \Delta \mathbf{x}^i, \quad i = 0, 1, \dots, \quad \mathbf{x}^0 = \mathbf{x}_k. \quad (16)$$

If eq.(15) is approximately fulfilled then use the solution as new point  $\mathbf{x}_{k+1}$ . The point is situated at an RGF curve with respect to direction  $\mathbf{r}_{k+1}$ . The key idea is that like in the former derivation of (6) we have now also assumed a ‘constant’  $\mathbf{P}_{\mathbf{x}'(\mathbf{t})}$  matrix, in the current step. This is here an approximation, but it works self-consistent. In the limit, this numerical procedure leads to the valley GE. The approximation of a ‘constant’  $\mathbf{P}_{\mathbf{x}'(\mathbf{t})}$  matrix allows us to avoid third derivatives of the PES.

## 5 Approximative Search for GEs to higher eigenvalues

The TASC method uses the property of the valley floor: the GE of the floor and a swath of RGF curves along the valley are nearly parallel. It is possible to calculate the floor GE by using an RGF curve to tangent direction  $\mathbf{t}$ . That property does not generally hold for higher GEs. RGF curves may intersect the GE to a higher eigenvalue under a large angle, in the limit up to  $90^\circ$ .

On the GE, there is the gradient  $\mathbf{g}$  an eigenvector  $\mathbf{e}_i$  of the Hessian. We search for a curve point where it is

$$\boxed{\mathbf{P}_{\mathbf{e}_i} \mathbf{g}(\mathbf{x}) = 0} \quad (17)$$

The equation is trivially fulfilled on the GE, and it is used for the corrector step. After the prediction of a point near the GE, we start with the  $\mathbf{e}_i$  of that point and use the corrector for eq. (17) to get point  $\mathbf{x}_1$ . Next we iteratively have to calculate the  $\mathbf{e}_i$  at a solution point  $\mathbf{x}_k$ ,  $k = 1, 2, \dots$  and repeat the corrector for eq. (17) up to convergence. Locally, at points near the GE, the method works.

The tangent of an RGF curve to the eigenvector  $\mathbf{e}_i$  cannot be used to get the predictor step, as it is possible with TASC or RGF itself, because the tangent of that curve usually is not near the tangent of the GE, if the GE follows a higher eigenvalue. A way out is a very simple predictor step using the secant step of the two previous points,  $\mathbf{x}_k$  and  $\mathbf{x}_{k-1}$ , of the GE:

$$\mathbf{d} = \mathbf{x}_k - \mathbf{x}_{k-1}, \quad \text{and} \quad \mathbf{x}_{k+1} = \mathbf{x}_k + \mathbf{d} . \quad (18)$$

The method is very cheap and works well. Note that we do not economize derivations of the gradient, because in order to solve eq. (17) by Newton-Raphson needs again second derivatives, or updates of the Hessian, like in RGF or TASC.

## 6 Conclusions and Perspectives

The IRC is the most used model of the reaction path . This is due to the following properties:

- (i) simplicity,
- (ii) computational economy,
- (iii) reproducibility, and
- (iv) conceptually free of error.

The simplicity (i) of the IRC is evident. For point (ii), there are sometimes convergence problems near the minimum on a flat valley floor, because the IRC shows an affinity to zigzagging, and (iii) needs a careful definition of the coordinate system. If there is a continuous valley from saddle point to minimum (convex isopotential hypersurfaces with respect to the minimum) the IRC may best serve as a reaction path model. However, in case of the existence of concave VRI regions along the reaction progress, point (iv) is generally not fulfilled. One has to look for other reaction path models or modifications which may bifurcate at the VRI point.

The new model should include the RGF approach, as well as the valley extremals, special GEs.

- Starting at a stationary point, one can follow the GE in a valley or cirque direction and search for the next VRI point.
- Beginning at this point (using the gradient at this point for the search direction) one can calculate the branches of the corresponding RGF curve and can assign the reaction path model to the branches which show the ‘good’ direction.

RGF fulfills (i) to (iii), however, the numeric GE calculation does not fit (ii). Therefore, we propose to calculate the pathways along any GE more simply. We use the evaluation of gradient and Hessian matrix per iteration step. The procedure is a new method for studying the GEs of a multidimensional hypersurface. The method is implemented as a separate FORTRAN shell. It will be distributed on request [#].

## Some References

[#] e-mail: [quapp@rz.uni-leipzig.de](mailto:quapp@rz.uni-leipzig.de)

Web: <http://www.mathematik.uni-leipzig.de/MI/quapp>

1. Quapp W, Heidrich D (1984) *Theoret Chim Acta* 66: 245-260
2. Quapp W (1989) *Theoret Chim Acta* 75: 447-460
3. Heidrich D, Kliesch W, Quapp W (1991) *Properties of Chemically Interesting Potential Energy Surfaces, Lecture Notes in Chemistry* 56, Springer, Berlin
4. Quapp W (1994) *J Chem Soc, Faraday Trans* 90: 1607-1609
5. Quapp W, Imig O, Heidrich D (1995) in: Heidrich D, ed., *The Reaction Path in Chemistry: Current Approaches and Perspectives*, Kluwer, Dordrecht, pp.137-160
6. Quapp W, Hirsch M, Imig O, Heidrich D (1998) *J Computat Chem* 19: 1087-1100
7. Quapp W, Hirsch M, Heidrich D (1998) *Theoret Chem Acc* 100: 285-299
8. Hirsch M, Quapp W, Heidrich D (1999) *Phys Chem Chem Phys* 1: 5291-5299
9. Quapp W, Hirsch M, Heidrich D (2000) *Theoret Chem Acc*, 105: 145-155
10. Quapp W, Melnikov V (2001) *Phys Chem Chem Phys* 3: 2735-2741
11. Quapp W (2001) *J Computat Chem* 22: 537-540
12. Quapp W, Heidrich D (2002) *J Mol Struct THEOCHEM* 585: 105-117
13. Hirsch M, Quapp W (2002) *J Computat Chem* 23: 887-894
14. Quapp W (2003) *Reduced Gradient Methods and their Relation to the Reaction Path, J. Theor. Comput. Chem.* accepted.